

Adsorption and decomposition of H_2NCHO , D_2NCHO , N_2H_4 , and NH_3 on $\text{Rh}(111)$ *

M.L. Wagner and L.D. Schmidt

Department of Chemical Engineering and Materials Science, University of Minnesota, Minneapolis, MN 55455, USA

Received 6 November 1990; accepted for publication 23 May 1991

The adsorption and decomposition of H_2NCHO , D_2NCHO , N_2H_4 , and NH_3 on $\text{Rh}(111)$ have been examined using TPD. Adsorption of H_2NCHO on $\text{Rh}(111)$ at 100 K produces four major desorption products: CO , H_2 , N_2 , and NH_3 . The absence of any CN bond retention demonstrates that CO bond formation is favored over CN bond formation on $\text{Rh}(111)$. At low coverage N_2 is the primary nitrogen containing product, but near saturation up to $\sim 25\%$ NH_3 is formed. Hydrogen desorption has a peak from the recombination of H adatoms and a reaction limited peak at ~ 450 K. The decomposition of D_2NCHO showed that the reaction-limited H_2 comes from the amino group, and mass balances support the assignment of the reacting species as NH. The stability of NH suggests that NH decomposition may be a limiting factor in NH_3 decomposition. Ammonia desorption from H_2NCHO was reaction-limited and appeared to be formed from the scavenging of H adatoms by a NH_2 surface species. Adsorption of N_2H_4 on $\text{Rh}(111)$ at 100 K gave rise to three major desorption products: N_2 , H_2 , and NH_3 . N_2 desorption has a peak at ~ 700 K formed by the recombination of N adatoms at ~ 700 K and also a low-temperature N_2 peak at ~ 270 K which was due to the decomposition of a N_2H_y ($y \leq 3$) species not involving the scission of the N–N bond. H_2 desorption from N_2H_4 results from the recombination of H adatoms and the decomposition of NH. NH_3 desorption from N_2H_4 has a peak corresponding with the NH_3 peak from H_2NCHO and a second peak caused by the direct intramolecular decomposition of N_2H_4 .

1. Introduction

As part of a continuing study of CN and CNO surface chemistry on noble metals, the decomposition of formamide, H_2NCHO , on $\text{Rh}(111)$ has been investigated. Previously, the decomposition reactions of C_2N_2 , CH_3NH_2 , CH_3NO_2 , and $\text{C}_2\text{H}_5\text{NO}_2$ on $\text{Rh}(111)$ and $\text{Pt}(111)$ have been examined [1–4]. These studies have been mainly concerned with the stability of the CN bond on transition metals because of its importance in HCN synthesis. These studies demonstrated that the CN bond is stable on $\text{Pt}(111)$ to ~ 1000 K [1–3] and on $\text{Rh}(111)$ to ~ 800 K [3,4]. On $\text{Pt}(111)$ all the CN bonds were retained following C_2N_2 and CH_3NH_2 adsorption [1], whereas on $\text{Rh}(111)$ at saturation only 80% of the CN bonds of C_2N_2

were retained and just 35% of the CN bonds from CH_3NH_2 were retained [4]. Significant amounts of CN bonds were also retained following the adsorption of CH_3NO_2 [2] and $\text{C}_2\text{H}_5\text{NO}_2$ [3] and $\text{Pt}(111)$, while adsorbing these compounds on $\text{Rh}(111)$ produced complete CN bond scission [3].

H_2NCHO is particularly interesting because it has two different potential decomposition mechanisms, one through CO bond scission with the retention of the CN bond, the other through CN bond scission with the retention of the CO bond. The stability of CO on transition metals is well documented, but on $\text{Pt}(111)$ and $\text{Rh}(111)$ the stability of the CN bond has also been demonstrated. The study of H_2NCHO decomposition therefore allows for the exploration of the effect of intramolecular oxygen on CN bonds. This is important for understanding the catalytic oxidation of CN species and the possible use of CNO species as HCN precursors.

* This research partially supported by DOE under Grant No. DE-F602-88ER13878-A02.

It will be shown that H_2NCHO decomposition on Rh(111) produces exclusively CO and NH_x surface fragments. Examining the surface reactions and stability of NH_x species is important in understanding the decomposition of NH_3 on transition metals and NH_3 oxidation in HNO_3 synthesis. Because NH_3 only decomposes on most transition metals at temperatures higher than the temperature that it desorbs, it has been difficult to study its surface decomposition fragments with standard surface science techniques. The creation of adsorbed NH_x species by H_2NCHO decomposition allows for such examination.

To more fully examine the surface chemistry of NH_x species on Rh(111), the adsorption and decomposition of hydrazine, N_2H_4 , and the adsorption and desorption of NH_3 were also studied. Of particular interest is the competition between the formation of N_2 and NH_3 following N_2H_4 decomposition. This competition is determined by the stability and reactions of NH_x species.

In this study the determination of the selectivity between the competitive decomposition routes has been of major interest. This information has been obtained using TPD as a quantitative tool. Careful desorption measurements have accurately measured the yields of all major decomposition products at coverages up to saturation. This had allowed for accurate determination of the selectivity of the Rh(111) surface for the various decomposition routes, the observation of the effects of coverage on the selectivity, and the elucidation of reaction mechanisms. Previous studies concerning the decomposition of H_2NCHO and N_2H_4 on transition metals have concentrated on the use of spectroscopies such as EELS and XPS to investigate surface intermediates with TPD only used peripherally. Due to the number and overlap of peaks in EELS, unequivocal peak assignments have been difficult to make, and previous studies have not determined selectivities and the effects of coverage on selectivities. This knowledge is required if the surface chemistry of these species is to be understood.

The adsorption and decomposition of H_2NCHO has previously been studied on Ru(001) [5,6], oxygen-precovered Ru(001) [6–8], and

Pt(111) [9]. On Ru(001), the main decomposition products observed were CO, N_2 , and H_2 , with trace amounts of NH_3 also detected. CO desorption was determined to be the first-order desorption of adsorbed CO. N_2 desorption was at high temperature and limited by the recombination of N adatoms. H_2 desorption included a TPD peak assigned to H adatom recombination, a peak assigned to the decomposition of NH, and several unassigned peaks. On Ru(001) precovered with a $p(1 \times 2)$ overlayer of oxygen adatoms, H_2NCHO also decomposed into CO, H_2 , and N_2 . CO and H_2 desorbed together in reaction-limited desorption peaks, and N_2 was formed by the recombination of N adatoms. The O adatom overlayer was left intact on the surface. On Pt(111), NH_3 , CO, and H_2 were observed as the major desorption products of H_2NCHO adsorption. A mass balance from these results indicates that either a second N-containing species must have also been formed, or that the observed H_2 desorption was mostly due to background H_2 .

The desorption and decomposition of N_2H_4 has been studied qualitatively on several transition metal surfaces [10–18], showing that N_2H_4 readily decomposes to form N_2 , H_2 , and NH_3 . Several studies also report multiple N_2 desorption peaks [10–12], multiple H_2 desorption peaks [11–14] and multiple NH_3 desorption peaks [14]. These studies demonstrate that the decomposition is complex, and, thus far, little work has been done to explain the selectivity to NH_3 and N_2 formation or to determine the probable reaction paths.

The adsorption and decomposition of NH_3 has been studied on many transition metal surfaces [19–30]. These studies indicate that on all of the surfaces, with the possible exception of Rh(110) [19] and Ru(1,1,10) [20], NH_3 adsorbs molecularly and desorbs intact by ~ 300 K. NH_3 decomposition has been observed on several transition metal surfaces when the surfaces have been exposed to NH_3 while being held at elevated temperatures (> 300 K) [19–24]. At high pressures, NH_3 undergoes oxidation at elevated temperatures on all noble metals. NH_3 oxidation at elevated temperatures has also been observed at UHV conditions over Pt(111) [31] and Pt(S)-12(111) \times (111) [31,32],

and at low pressures (0.1–1 Torr) over Pt, Pd, and Rh wires [33,34].

2. Experimental

All of the experiments were performed in a single UHV chamber which has been described previously [1]. The system has two leak valves, one of which is attached to a tube doser which could be used to direct gas onto both sides of the crystal ~ 1 cm from its surface in order to reduce background pressure. However, an important limitation of the tube doser is that it cannot be used to dose readily condensable species because such species condense in the doser and produce uncontrollable doses. This tube doser was therefore only used to dose NH_3 , H_2 , D_2 and CO. The second leak valve which dosed through conventional backfilling was used for H_2NCHO , D_2NCHO , and N_2H_4 .

The Rh(111) crystal was a disc 0.8 cm in diameter oriented within 0.5° of the (111) crystal plane. The crystal was cleaned daily by first heating the crystal to 1500 K while dosing with 1×10^{-6} Torr of O_2 for 30 min and then heating to 1750 K in vacuum for 15 min. After such treatment the absence of surface impurities was confirmed by AES. AES was also used to examine the surface after desorption spectra were taken to search for any remaining surface C, O, and N. In TPD the crystal temperature was typically ramped at 20 K/s.

H_2NCHO of $> 99\%$ purity was further purified through several freeze–thaw–pump cycles. Because H_2NCHO is hygroscopic, water was a major contaminant, and, since the freezing point of water is near that of H_2NCHO , it was difficult to remove the water through the freezing cycles. To completely remove water, the sample was continually pumped by a turbomolecular pump during dosing. The doubly deuterated formamide, D_2NCHO , was obtained from MSD Isotopes with 99.9% D.

Anhydrous N_2H_4 of 98% purity was further purified by several freeze–thaw–pump cycles. To create a reservoir of N_2H_4 for dosing, the gas

handling system was first evacuated with a turbomolecular pump, purged with the vapor of the N_2H_4 sample, isolated from the pump, allowed to fill with N_2H_4 vapor, and finally isolated from the N_2H_4 liquid sample. It was found that the N_2H_4 in the dosing reservoir would degrade, and therefore this procedure was repeated several times a day to replace the N_2H_4 . Anhydrous NH_3 was used without further purification. The purity of each of the dosing species was monitored during dosing using the mass spectrometer in the UHV chamber.

The coverages of desorbing H_2 and NH_3 were determined by normalizing the desorption peak areas with the respective desorption peak areas following saturating exposures of H_2 and NH_3 . The saturation coverage of H_2 was taken to be 8×10^{14} molecules/cm² based on H_2 desorption following H_2 adsorption on Rh(111) at 100 K [35], and the saturation coverage of NH_3 was taken to be 3.8×10^{14} molecules/cm² based on NH_3 desorption following NH_3 adsorption on Pt(111) at 100 K [20].

Mass 12 and mass 14 were monitored for CO and N_2 desorption, respectively, in order to differentiate between CO and N_2 . To determine the CO and N_2 coverages, the mass 12 and mass 14 peak areas were first transformed into mass 28 peak areas by dividing by the mass 12 cracking fraction exhibited by CO and the mass 14 cracking fraction exhibited by N_2 . The CO coverage was calibrated by saturation exposure of CO with the saturation coverage of CO assumed to be 1×10^{15} molecules/cm² based on CO desorption following CO adsorption on Rh(111) at 300 K [36]. It was assumed that N_2 possessed the same sensitivity in the mass spectrometer and the same pumping speed in the UHV chamber as CO, so the same normalization was used for N_2 .

In order to compare directly the yields of H_2 , D_2 , and HD, following the decomposition of D_2NCHO , the mass spectrometer sensitivities of the three species were obtained. Because H_2 and D_2 adsorption produce the same saturation coverage, the comparison between the TPD peak areas following saturation doses of H_2 and D_2 reveals the relative mass spectrometer sensitivities. The H_2/D_2 sensitivity ratio was found to be

1.51, and the H_2/HD sensitivity ratio was assumed to be 1.26.

Long pump-down times (> 10 min) were caused by the low pumping speed of H_2NCHO and N_2H_4 . These long pump-down times produced some exposure from background CO, H_2 , and residual amounts of the dosing species. In determining product yields following H_2NCHO and N_2H_4 exposures, care was taken to subtract out this background desorption by obtaining repeated background spectra. For H_2NCHO , the background was found to be nearly constant and was easily accounted for. H_2 proved to be the only significant background contaminant and contributed approximately 30% of the H_2 signal at saturation. For N_2H_4 , background desorption from H_2 and NH_3 was significant and increased with increasing exposure. This background desorption was due to the formation of these species by the unavoidable partial decomposition of N_2H_4 to form NH_3 , H_2 , and N_2 prior to performing TPD. This partial decomposition occurred either on the walls of the UHV chamber, the walls of the gas handling system, the hot filaments in the UHV chamber, or the Rh(111) surface at 100 K.

3. Results

3.1. Formamide

Spectra of all the observed desorption products following 5 L of H_2NCHO at 100 K are shown in fig. 1. This shows that the sole carbon- and oxygen-containing decomposition species is CO. Nitrogen is seen to desorb as both NH_3 and N_2 . Hydrogen desorbs as NH_3 and H_2 . The figure also shows the desorption of a small amount of undecomposed molecular H_2NCHO . Mass 28 spectra gave results completely consistent with the CO and N_2 desorption peaks. Masses 16, 18, 26, 27, 32, 44, and 52 were also monitored, but produced either no peaks or peaks that were the cracking fragments of the desorption products noted above. Details concerning each of these desorption products are discussed individually below.

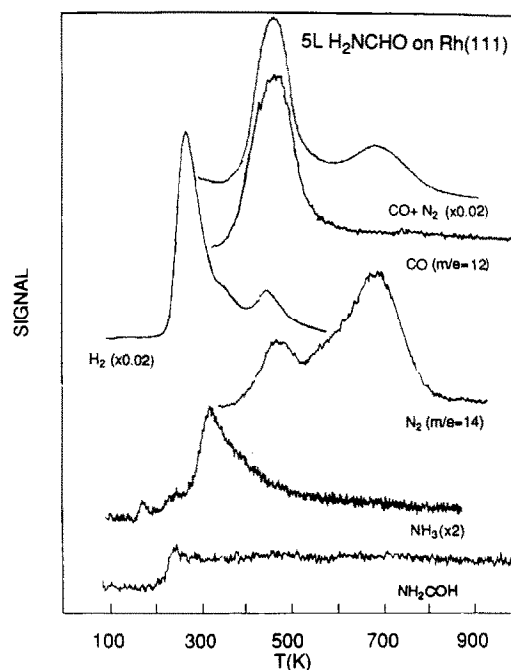


Fig. 1. Survey of the TPD spectra of all the major desorption species following the adsorption of 5 L of H_2NCHO on Rh(111) at 100 K.

Fig. 2a presents CO desorption spectra ($m/e = 12$) taken following H_2NCHO exposures up to saturation, following adsorption at 300 K. Spectra were also taken following adsorption at 100 K, and gave results identical to those presented in fig. 2a. AES spectra taken following dosing with H_2NCHO and then flashing the crystal temperature to 1000 K showed no carbon or oxygen ($< 1\%$ of saturation) remaining on the surface.

The CO desorption occurs between 400 and 600 K. The peak maximum shifts from 510 to 485 K with increasing coverage, but despite this downshift the peak is the first-order desorption-limited desorption of CO. This is evident since the first-order desorption-limited desorption of CO following molecular CO exposures on Rh(111) occurs near 500 K [32]. This is shown in fig. 2b. The unusual downshift of the CO desorption temperature with increasing coverage may be explained by the buildup of N adatoms. The somewhat electronegative N adatoms may withdraw electron density from the surface Rh atoms, reducing the effect of surface back bonding into the

$CO 2\pi^*$ antibonding orbital, lowering the metal-CO bond strength, and thereby decreasing the desorption temperature. A similar mechanism was used to explain similar effects observed on $Ru(001)$ following H_2NCHO adsorption [5] and following CO coadsorption with ordered oxygen adatom overlayers [37].

Fig. 3a shows N_2 desorption spectra following various H_2NCHO exposures up to saturation. The smaller peaks centered near 500 K are due to cracking from CO desorption. N_2 desorption forms a broad peak occurring between ~ 550 and ~ 900 K. The peak maximum shifts down with increasing coverage from 755 to 693 K. The desorption temperature of this peak and its shift with increasing coverage is consistent with the second-order reaction-limited recombination of N adatoms. Similar broad high temperature N_2 peaks have been observed on $Rh(111)$ following NO adsorption [38], HNCN adsorption [39], CH_3NO_2 adsorption [3], and $C_2H_5NO_2$ adsorption [3]. These peaks have all been designated as arising from N adatom recombination. For com-

parison, the N_2 peaks arising from CH_3NO_2 decomposition (from [3]) are shown in fig. 3b.

As shown in fig. 4a, following low H_2NCHO exposures (< 0.1 L), NH_3 is seen to desorb as a small broad peak centered at ~ 320 K. At higher coverages (0.5 L), a shoulder near 400 K develops, while at still higher coverages, the original peak and the shoulder are no longer distinguishable and form a single asymmetric peak with a maximum at ~ 320 K. At 5 L a small shoulder develops at ~ 250 K. NH_3 desorption spectra following NH_3 adsorption are shown in fig. 4b. Comparison between figs. 4a and 4b demonstrates that the NH_3 desorption following H_2NCHO adsorption must be reaction-limited.

Fig. 6a shows that the amount of nitrogen going to NH_3 more than doubles from low coverage to saturation. At low coverages less than 10% of the nitrogen adsorbs as NH_3 , while at saturation approximately 25% of the nitrogen desorbs as NH_3 . Fig. 6a also shows the C/N (including N_2 and NH_3) ratio to be very nearly 1 (1.06 ± 0.04).

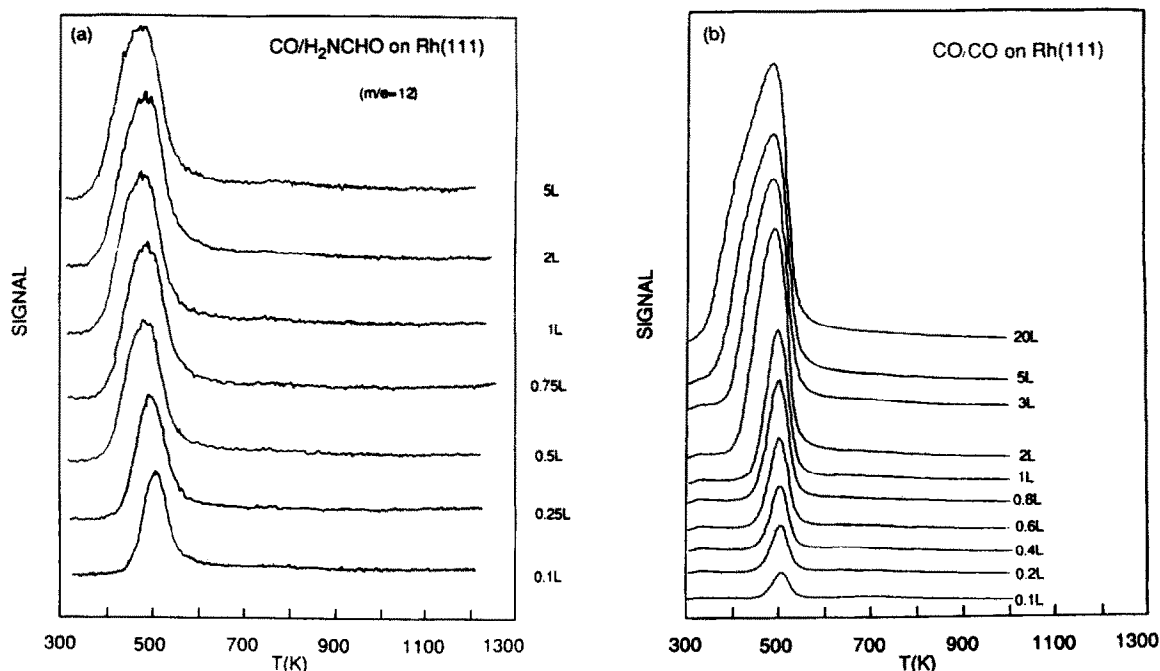


Fig. 2. TPD spectra of (a) CO desorption ($m/e = 12$) following the adsorption of H_2NCHO on $Rh(111)$ at 300 K, and (b) CO desorption ($m/e = 28$) following the adsorption of CO on $Rh(111)$ at 300 K.

Fig. 5a shows H_2 desorption spectra following H_2NCHO adsorption at 100 K up to an exposure of 3 L. Higher-exposure TPD spectra up to satu-

ration were also taken but showed no more shifts in peak temperature or relative peak size. At low coverages a desorption peak occurs at 370 K and

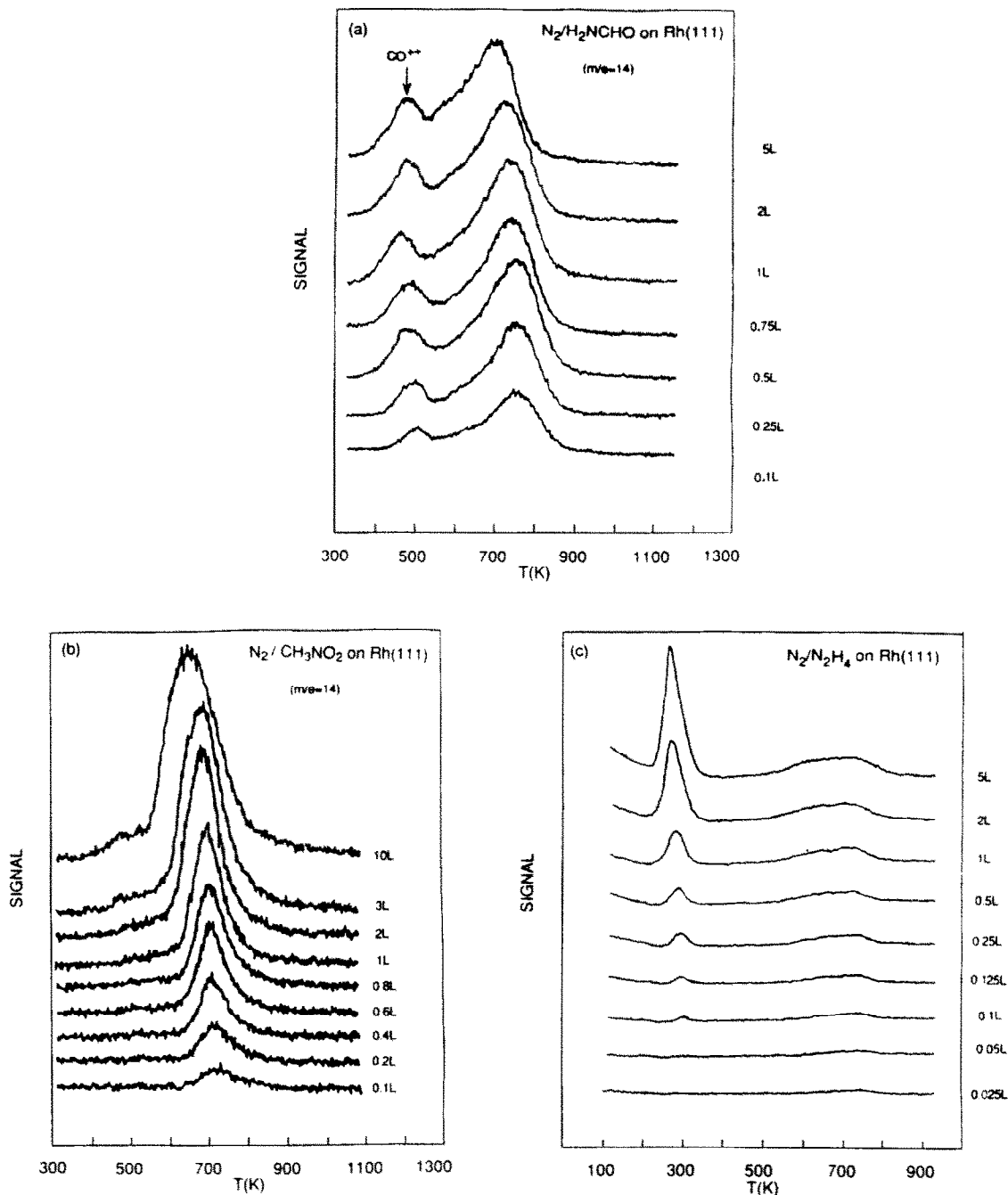


Fig. 3. TPD spectra of N_2 desorption ($m/e = 14$) following the adsorption of (a) H_2NCHO on Rh(111) at 300 K, (b) CH_3NO_2 on Rh(111) at 300 K [3], and (c) N_2H_4 on Rh(111) at 100 K.

shifts down with increasing coverage to 310 K at 1.6 L. At still higher coverages this peak narrows and shifts further down to 280 K, revealing a

small shoulder at 365 K. Significant amounts of H_2 desorption due to the adsorption of background H_2 were unavoidable. This background is

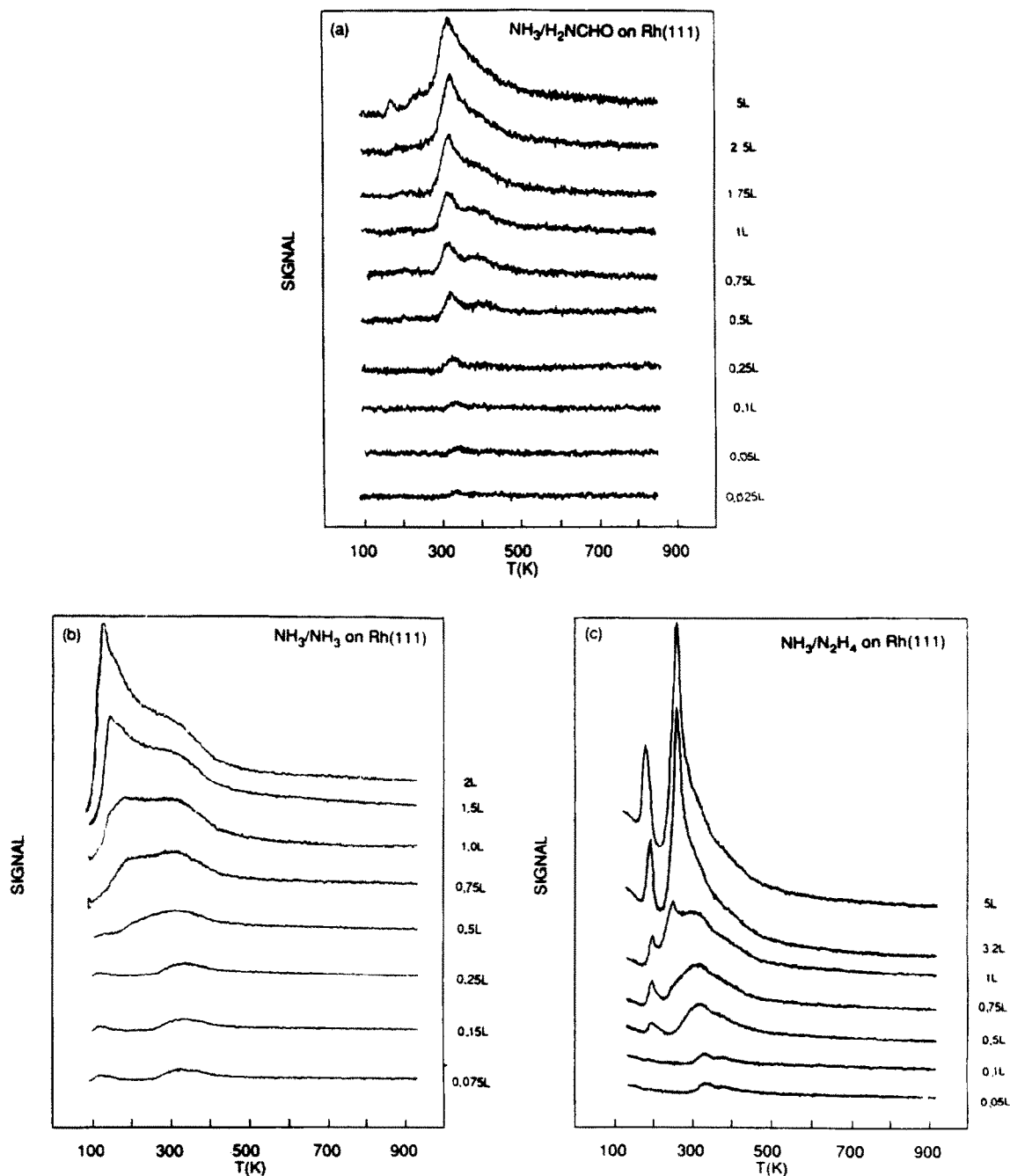


Fig. 4. TPD spectra of NH_3 desorption following the adsorption of (a) H_2NCHO , (b) NH_3 , and (c) N_2H_4 on Rh(111) at 100 K.

shown in the spectra but is subtracted in all the relevant mass balances. At low coverages the major H_2 peak is also seen to possess a small

high temperature shoulder which quickly develops into a separate higher temperature peak. This high temperature peak has a maximum which

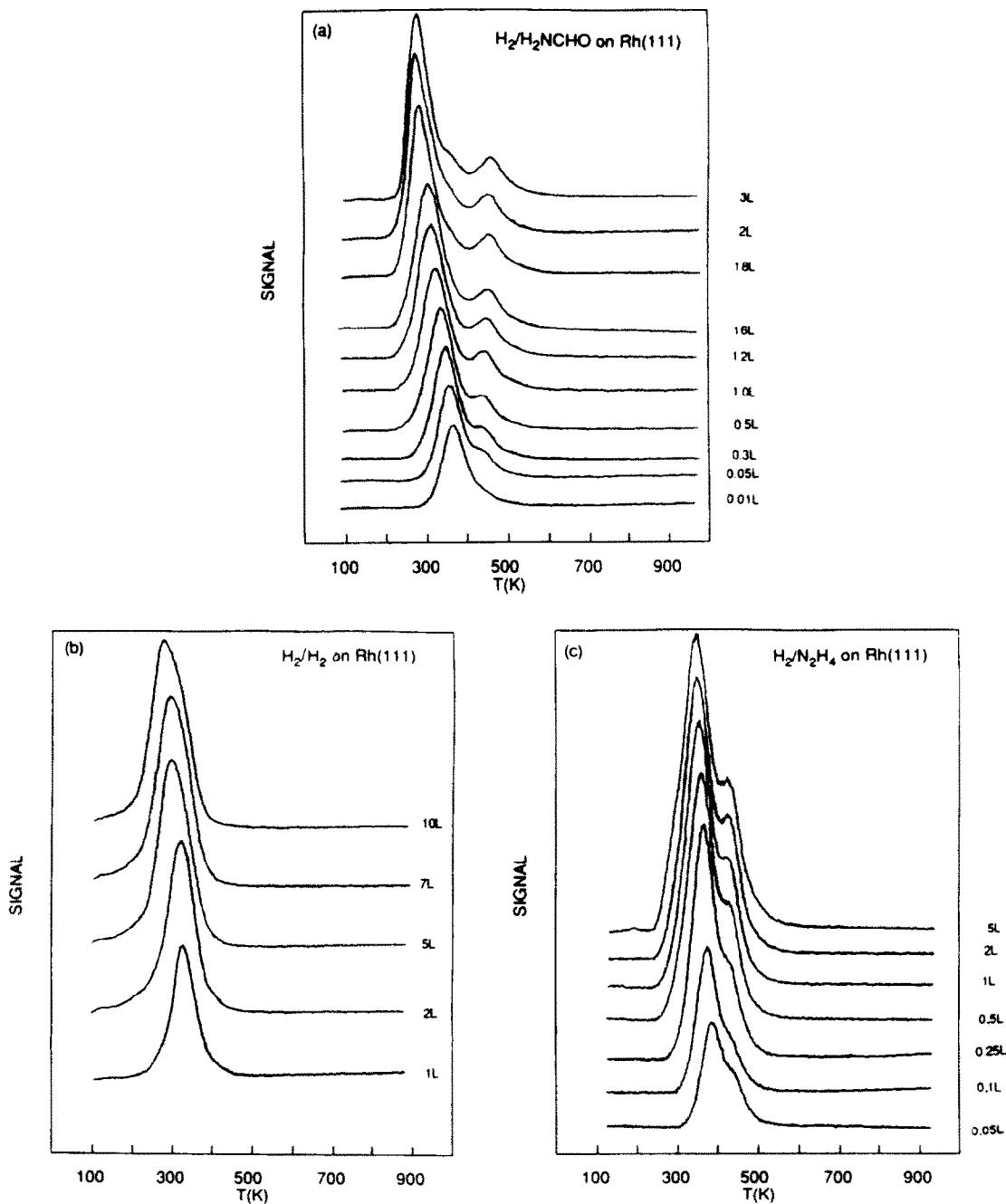


Fig. 5. TPD spectra of H_2 desorption following the adsorption of (a) H_2NCHO , (b) H_2 , and (c) N_2H_4 on Rh(111) at 100 K.

shifts up from 440 to 456 K with increasing coverage. For comparison, H_2 desorption spectra following H_2 adsorption are shown in fig. 5b. The low-temperature H_2 desorption peak is consistent with the recombination of H adatoms which is observed following H_2 adsorption on Rh(111) [31]. The high-temperature desorption peak must then be reaction-limited desorption of H_2 following the decomposition of surface fragments.

The mass balance between the total hydrogen desorption (including H_2 and NH_3), and the CO desorption shows a H/C ratio very near 3 (2.91 ± 0.09) at all coverages, as expected. Also, a mass balance between the reaction-limited H_2 desorption and the N_2 desorption showed a H/N ratio near 1 (1.08 ± 0.02). A mass balance between the low-temperature H_2 desorption and the reaction-limited H_2 desorption showed a ratio near 2 (1.88 ± 0.17). Assignment of the reaction-limited H_2 peaks is discussed later along with the results from the study of D_2NCHO .

Molecular H_2NCHO desorbs in a single sharp desorption peak at 247 K (data not shown). This peak develops after the other desorption product peaks saturate and does not itself saturate. Therefore this peak is a multilayer ice peak.

The uptake curve for the four desorbing species is shown in fig. 6a. The saturation coverage for H_2NCHO can be based on CO since every H_2NCHO molecule which adsorbs on the surface (up to saturation) produces one CO molecule. This gives a saturation coverage of 3.9×10^{14} molecules/cm². Based on CO, the uptake curve also indicates a sticking coefficient of 0.5 for H_2NCHO .

3.2. Deuterated formamide

The decomposition of D_2NCHO was investigated to determine the source of the H_2 peaks and investigate the NH_3 formation mechanism. Results of H_2 , HD, and D_2 desorption at two coverages are shown in fig. 7. In this figure, the D_2 and HD spectra have been normalized with respect to the H_2 spectra to account for the different mass spectrometer sensitivities and allow for a direct comparison between the peaks. The dotted spectra are estimates of the H_2 de-

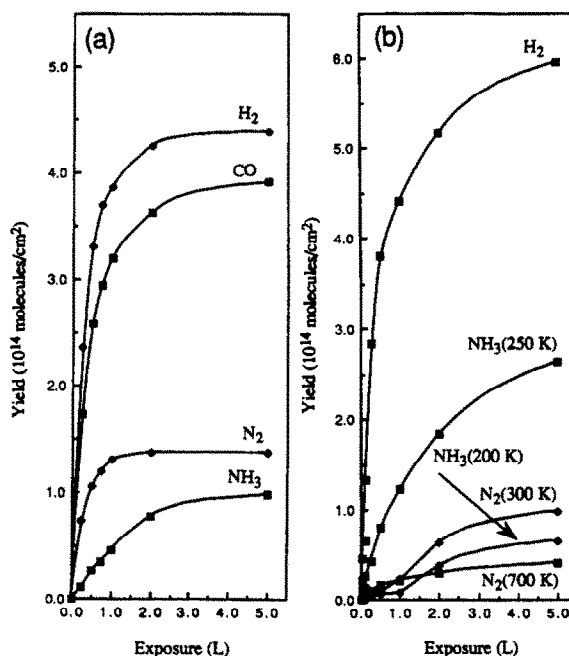


Fig. 6. Decomposition product yields as a function of exposure of (a) H_2NCHO and (b) N_2H_2 following the adsorption of the parent species on Rh(111) at 100 K.

sorption after the H_2 from the adsorption of background H_2 was subtracted.

When the additional H adatoms coming from the background adsorption of H_2 are included, the equilibrium distribution among the isotopes indicates that an $H_2/HD/D_2$ ratio of approximately 0.35/0.48/0.17 should be observed for the 0.5 L spectra and a ratio of approximately 0.33/0.49/0.19 should be observed for the 2.5 L spectra. Fig. 7 demonstrates that this is clearly not the case.

H_2 desorption dominates the low-temperature peak. This peak is due to the recombination of hydrogen adatoms. The lack of any major H_2 desorption in the high-temperature peak indicates that nearly all of the formyl H desorbs in the lower peak. Also desorbing in this peak are the H adatoms from the H_2 background and some D adatoms. The presence of the D adatoms shows that some of the amino hydrogens form adatoms. Since the D adatoms are in an environment dominated by H adatoms, the D desorbs primarily as HD rather than D_2 .

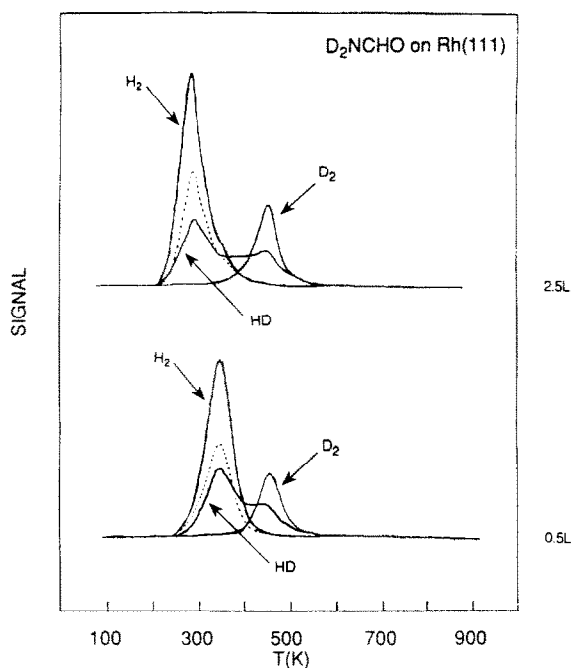


Fig. 7. TPD spectra of H_2 , HD, and D_2 following the adsorption of D_2NCHO on Rh(111) at 100 K after a 0.5 L and a 2.5 L exposure. The HD and D_2 spectra have been normalized with respect to the H_2 spectra to account for differing mass spectrometer sensitivities. Significant amounts of H_2 and HD desorption are due to the adsorption of background H_2 . Dotted spectra represent the amount of the H_2 after background H_2 has been subtracted.

D_2 desorption dominates the high-temperature peak. This indicates that the reaction-limited hydrogen comes almost completely from the amino group. The HD in the high-temperature peak is due to the tail of the desorption peak due to the recombination of H adatoms (as evidenced by the H_2 desorption spectra) extending into the high-temperature peak. In this temperature range, the remaining H adatoms are surrounded by the D adatoms and primarily desorb in the form of HD.

Even with the background H_2 subtracted, the D/H ratio for both coverages was found to be 1.2, lower than the expected value of 2. This may be due to a systematic error among the assumptions needed to calculate the D/H ratio or due to exchange with background H_2 . Still, the data clearly shows that the lower-temperature H_2 desorption peak following the decomposition of

H_2NCHO is due to the recombination of H adatoms formed by the dehydrogenation of the formyl group and the partial dehydrogenation of the amino group and that the reaction-limited H_2 is due to the decomposition of an NH_x species. The exact nature of this NH_x species is discussed later.

Significant amounts of NDH_2 , ND_3 , and ND_2H desorption (data not shown) were all detected following exposures of 0.1, 1, and 5 L of D_2NCHO . Since the mass spectrometer showed that no D_2NCDO was dosed, the ND_3 must be formed by an intermolecular surface reaction (an intramolecular reaction could only produce ND_2H). This indicates that at least a portion of the ammonia formation reaction must be intermolecular.

3.3. Hydrazine

Desorption spectra from all the significant species detected desorbing from the Rh(111) surface following a saturation exposure of N_2H_4 at 100 K are shown in fig. 8. The only desorption products observed were N_2 , H_2 , and NH_3 . The N_2 is seen to desorb in two peaks: a broad peak with a maximum at 705 K and a sharper lower-temperature peak at 273 K. The mass 14 cracking fragment of N_2 was monitored instead of mass 28 so that desorption from background CO would not interfere. H_2 is seen to have two largely overlapping desorption peaks, one peak is centered at 350 K and the other near 430 K. The NH_3 desorbs in two sharp asymmetrical peaks. The major peak has a maximum at 250 K, and the smaller peak maximum is at 180 K.

N_2 (mass 14) desorption peaks following the adsorption of N_2H_4 at 100 K are shown in fig. 3c. At coverages less than 0.1 L only a shallow broad desorption peak between ~ 600 K and ~ 800 K with a maximum near 750 K is observed. At 0.1 L a low-temperature N_2 peak at 309 K is seen to develop. With increasing coverage, both peaks continue to grow. However, the low-temperature peak grows at a larger rate. Also, with increasing coverage the high-temperature peak broadens to begin at ~ 500 K and shifts its maximum from 750 to 710 K, while the low-temperature peak

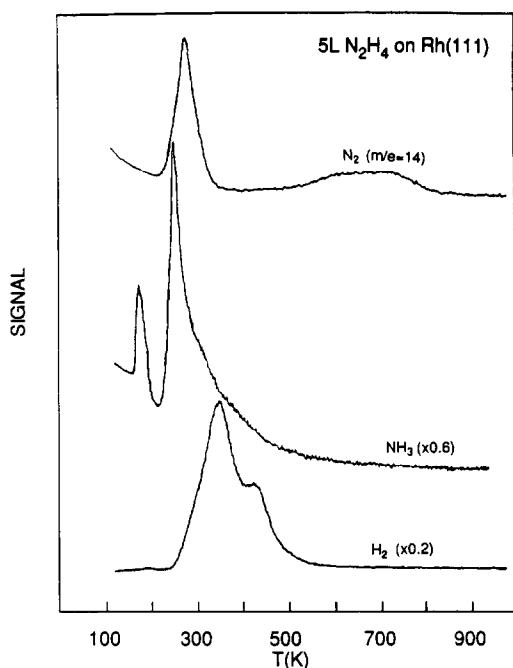


Fig. 8. Survey of the TPD spectra of all the major desorption species following the adsorption of N_2H_4 on Rh(111) at 100 K.

shifts down to 273 K. Similar low-temperature N_2 desorption has been observed following the adsorption of N_2H_4 on Ir(111) [10], polycrystalline Ir foil [11], and polycrystalline Rh foil [12]. Like H_2NCHO and CH_3NO_2 [3], the desorption temperature of the high-temperature N_2 peak and its down-shift with increasing coverage are consistent with the second-order reaction-limited recombination of N adatoms. The symmetry and temperature shift of the low-temperature peak appear to be consistent with a second-order peak, although it is possible that the temperature shift might be caused by repulsive adsorbate interaction. Since N adatoms do not recombine until above 500 K, the low-temperature peak can not be due to the recombination of N adatoms. Also, since molecular N_2 does not adsorb on Rh(111) at 100 K, the low-temperature N_2 peak cannot be the desorption of adsorbed N_2 . The low-temperature formation of N_2 must then be the decomposition of or reaction between a N_xH_y species. The most probable species is a partially dehydrogenated N_2H_4 fragment, N_2H_y ($y \leq 3$).

Desorption spectra of NH_3 following the adsorption of N_2H_4 at 100 K are shown in fig. 4c. At low coverage (0.05 and 0.1 L) NH_3 is seen to desorb in a shallow peak with a maximum near 320 K and a shoulder near 400 K. At 0.5 L, the original NH_3 peak grows larger and a second peak at 200 K begins to develop. At 0.75 L, a low-temperature shoulder develops at 250 K while the 200 K peak continues to grow. At 1 L the 250 K shoulder begins to develop into a sharp peak. At higher coverages, the 250 K peak grows to dominate the high-temperature NH_3 desorption, and the low-temperature NH_3 peak continues to grow and shifts down to 180 K. A similar NH_3 spectrum with peaks at 150 and 270 K was observed following the adsorption of N_2H_4 on Rh(100) [14].

A comparison of fig. 4c with 4b shows that all of the NH_3 desorption from N_2H_4 adsorption is reaction-limited. A comparison of fig. 4c and 4a shows that at low coverages (≤ 0.5 L) the high-temperature NH_3 desorption following the adsorption of N_2H_4 closely resembles NH_3 desorption following H_2NCHO . At 0.75 L, a low-temperature shoulder at 250 K is added to the high-temperature NH_3 peak. Following a saturation exposure of H_2NCHO , a similar shoulder at 250 K is seen to develop. At the exposures where the 250 K shoulder first develops, the NH_3 yields are similar for the two different adsorbates (0.98×10^{14} molecules/cm² for H_2NCHO and 0.87×10^{14} molecules/cm² for N_2H_4). This suggests that an identical mechanism is causing the (high-temperature) formation of NH_3 from both adsorbates. Possible mechanisms for the NH_3 formation are discussed later.

Fig. 5c shows H_2 desorption spectra following the adsorption of N_2H_4 at 100 K. At low coverages (< 0.5 L), the H_2 desorbs in a single major peak which starts at 370 K (at 0.05 L) and shifts down to 361 K (at 0.25 L). This peak also has a shoulder near 430 K. As the coverage increases, the shoulder develops into a separate peak with its maximum remaining at 430 K, and the lower-temperature peak continues to grow while shifting down to 350 K. The lower-temperature H_2 peak is consistent with the H_2 peak arising following H_2 adsorption (fig. 5b), and is therefore

due to the recombination of H adatoms. The higher-temperature H_2 peak is reaction-limited and must be caused by the decomposition of a N_xH_y species.

The uptake curves for the two N_2 peaks, the two NH_3 peaks, and the total H_2 content are shown in fig. 6b. The H_2 peaks are not entered separately due to the inability to accurately deconvolute the two peaks. The partial decomposition of the N_2H_4 prior to performing TPD results in additional H_2 desorption and some additional NH_3 desorption. Assuming only minor NH_3 contamination, the saturation coverage for N_2H_4 can be based on half the total N coverage (including NH_3 and N_2) since every N_2H_4 molecule which adsorbs on the surface produces two N atoms. This indicates a saturation coverage of 3×10^{14} molecules/cm². Fig. 6b shows that the fraction of total N for each of the four N-containing species varies significantly with coverage. The fractions of N in the high-temperature N_2 peak and high-temperature NH_3 peak decrease with increasing coverage, whereas the fractions in the low-temperature peaks increase with increasing coverage.

3.4. Ammonia

Fig. 4b shows NH_3 desorption following the adsorption of NH_3 on $Rh(111)$ at 100 K. At low exposures (< 0.25 L), NH_3 desorbs intact in a broad peak between ~ 275 and ~ 425 K. At higher doses, a second desorption peak is seen to develop at 160 K. Finally, after 1.5 L exposure, an NH_3 ice peak develops at 140 K. This peak was found to grow without saturation at higher coverages. No decomposition fragments are observed at any coverage. This behavior is consistent with that observed for NH_3 adsorption at 100 K on other metals such as $Pt(111)$ [21,26] and $Ru(001)$ [20].

4. Discussion

4.1. Formamide decomposition

H_2NCHO decomposes on $Rh(111)$ to form CO, H_2 , N_2 , and NH_3 . The N_2 formation occurs

completely through the recombination of N adatoms. The source of the N adatoms appears to be the decomposition of NH surface fragments. This assignment is supported by several facts. First, the D_2NCHO experiments show that the reaction-limited H_2 desorption comes almost entirely from the amino group of the H_2NCHO , indicating that the high-temperature H_2 peak must be formed from the decomposition of a NH_x species. Second, the mass balance between the H_2 from NH_x decomposition and N_2 desorption showed a reaction-limited $H_2:N_2$ ratio near unity. Since every NH_x species upon decomposition must form a N adatom, this strongly suggest the NH species. Third, the mass balance between the low-temperature H_2 and the H_2 from NH_x decomposition showed a nearly two-to-one ratio. This is what would be expected if the reaction-limited H_2 were from NH and all the remaining H_2 desorbed in the lower-temperature peak. This assignment is also supported by data from H_2NCHO decomposition on $Ru(001)$ [5]. Parmeter et al. observed a reaction-limited H_2 desorption peak from H_2NCHO decomposition on $Ru(001)$ which had an upward shift in temperature with coverage (from 405 to 410 K). From studying the adsorption and decomposition of D_2NCHO and employing EELS, this reaction-limited H_2 desorption peak on $Ru(001)$ was shown to be caused by the decomposition of NH. The desorption temperature of the reaction-limited H_2 peak following H_2NCHO decomposition on $Rh(111)$ shows a similar increase (from 440 to 455 K).

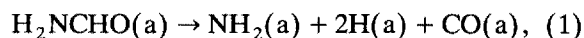
The increase in desorption temperature with increasing coverage for the reaction-limited H_2 suggests an increase in the binding energy of the NH fragments. This behavior could be explained by attractive interactions between adsorbed NH. Since amines are known to exhibit strong hydrogen bonding among themselves, hydrogen bonding between the adsorbed NH species could account for these attractive interactions.

NH_3 formation begins as a minor reaction and becomes increasingly important with increasing coverage. At low coverages less than 10% of the nitrogen desorbs as NH_3 , while at saturation approximately 25% of the nitrogen desorbs as NH_3 .

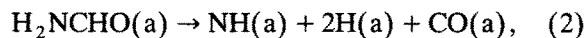
Results from H₂NCHO and N₂H₄ decomposition suggest that a common mechanism is behind the high-temperature formation of NH₃ from both adsorbates. Since N₂H₄ and H₂NCHO are distinctly different molecules, an intramolecular mechanism appears doubtful. The most probable mechanism is an intermolecular reaction involving the scavenging of H adatoms by NH_x species. Since it appears that NH is stable on Rh(111) up to ~ 450 K, the NH_x species forming NH₃ should be NH₂. The NH₃ formation reaction is therefore assigned to the scavenging of surface H by NH₂. The results from D₂NCHO decomposition also lends support to this assignment. An intramolecular decomposition reaction would be expected to produce almost entirely ND₂H, whereas an intermolecular reaction would produce a mixture of NDH₂, ND₃, and ND₂H. Following D₂NCHO decomposition, significant amounts of NDH₂, ND₃, and ND₂H desorption were all detected. At higher coverages, the NH₃ desorption peak remains unchanged while the H₂ peak due to the recombination of H adatoms shifts down to 270 K. This implies that either NH₂ formation or the stability of the NH₂ is the limiting step in the H adatom scavenging mechanism. It is possible that the presence of some H adatoms from the adsorption of background H₂ may have a minor effect on the selectivity of this reaction.

The increase in the relative production of NH₃ implies that the NH formation reaction becomes less favorable when compared to the NH₃ formation reaction. Thus, it appears that at low coverages the full dehydrogenation of the NH₂ group through the stable NH intermediate is favored, but, as coverage increases, this mechanism becomes less favorable, and the alternate path of rehydrogenating the NH₂ group to NH₃ becomes significant.

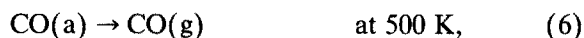
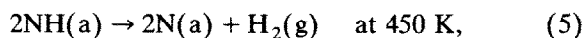
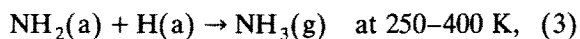
The decomposition path for H₂NCHO on Rh(111) is then:



and:



followed by:



In H₂NCHO decomposition on Rh(111) there is complete CN bond scission. However, the decomposition of CH₃NH₂ (a non-oxygen-containing CN bond analog to H₂NCHO) on Rh(111) produces only 65% CN bond scission even at saturation [4]. Thus, the addition of oxygen into CH₃NH₂ in the form of H₂NCHO activates complete CN bond scission. This behavior is explained by the great stability of CO on transition metals which causes complete CN bond scission below 500 K, the CO desorption temperature. To maintain the CN bond while decomposing the H₂NCHO molecule, the CO bond would have to be broken. This implies that N-CO bond containing species would probably not be good precursors for CN synthesis reactions. It also implies that in CN bond oxidation over Rh, the limiting factor must be the insertion of the oxygen into the CN-containing species since, once inserted, it appears that CN bond scission occurs easily.

In H₂NCHO decomposition on Ru(001), Parmeter et al. report that at saturation approximately 13% of the nitrogen goes toward NH₃ production [5]. This is significantly smaller than the 25% observed on Rh(111) at saturation. Flores et al. report that NH₃ is the major nitrogen-containing decomposition product formed following H₂NCHO decomposition on Pt(111) [9]. These results imply that the surface strongly affects the selectivity between N₂ and NH₃ production in H₂NCHO decomposition. The most aggressive of the three surfaces, Ru(001), appears to favor more strongly the complete dehydrogenation of the amino group to form N adatoms (which later combined as N₂), the less aggressive Rh(111) surface allows for more hydrogenation to NH₃, and the least aggressive surface, Pt(111), actually favors NH₃ production over N₂ production.

4.2. Hydrazine decomposition

The high-temperature N_2 formation is limited by the recombination of N adatoms. The presence of the N adatoms indicates that scission of the N–N single bond followed by the dehydrogenation of the resulting NH_x surface fragments must occur before high-temperature N_2 formation. The reaction-limited H_2 desorption peak at 430 K demonstrates that the decomposition of NH_x surface fragments occurs at this temperature. This reaction-limited H_2 peak occurs near the desorption temperature of the reaction-limited H_2 desorption peak that follows the decomposition of H_2NCHO on Rh(111). Since the reaction-limited H_2 peak from H_2NCHO has been assigned to the decomposition of NH, this strongly suggests that reaction-limited H_2 from N_2H_4 is also due to NH decomposition.

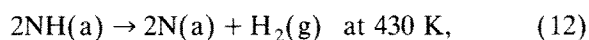
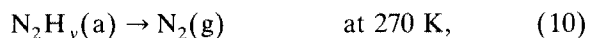
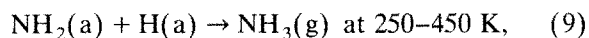
The low-temperature N_2 is probably caused by the reaction and/or decomposition of a N_2H_y ($y \leq 3$) surface species. Other possible species could be hydrazoic acid (N_3H) or a surface azide (N_3). Since H_2NCHO decomposition on Rh(111) does not produce a low-temperature N_2 peak, NH_2 and NH species (both of which occur in H_2NCHO decomposition) must be ruled out as possible reactants. Since NH_3 adsorption on Rh(111) does not produce a low-temperature N_2 peak, NH_3 must also be eliminated from consideration as the source of the low-temperature N_2 .

As explained above, it appears that the high-temperature NH_3 desorption from N_2H_4 and the NH_3 desorption from H_2NCHO have an identical mechanism: the scavenging of H adatoms by NH_2 surface fragments. The 250 K shoulder on the NH_3 peak from N_2H_4 begins to develop at an adsorbate coverage lower than the adsorbate coverage at which the shoulder on the NH_3 peak from H_2NCHO develops due to the greater amount of NH_2 and/or H adatoms formed by N_2H_4 . At higher coverages, following N_2H_4 adsorption, the 250 K shoulder continues to grow due to the continued availability of NH_2 and/or H adatoms and develops into a sharp peak that dominates the high-temperature NH_3 desorption. Due to the low coverage caused by surface saturation, the shoulder which starts to develop fol-

lowing H_2NCHO exposure is unable develop in the same fashion.

The low-temperature NH_3 peak is unique to N_2H_4 and must be caused by a second NH_3 formation reaction. Given the structure of the N_2H_4 molecule, with each N atom only bound to two H atoms, the low-temperature reaction must still be a H scavenging reaction. It is proposed that the low-temperature mechanism is the internal scavenging of a molecularly bound H in an intramolecular decomposition. In this mechanism, NH_3 is formed directly from N_2H_4 without first going through the NH_2 intermediate. Some of the NH_3 desorption in the temperature range between ~ 275 and ~ 400 K may also be due to the adsorption of background NH_3 .

The surface reactions which produce gas-phase products following the decomposition of N_2H_4 on Rh(111) are represented below with only the gas phase products shown. Many of the reactions would also produce N_xH_y , N, and H surface fragments. There may, of course, also be surface reactions which do not result in gas phase desorption.



4.3. Stability of NH_x species

The NH species is stable on Rh(111) until ~ 450 K and does not seem to hydrogenate in the presence of H adatoms to form either NH_2 or NH_3 . It is also more tightly bound on Rh(111) than NH_3 which desorbs from the surface by ~ 425 K. In contrast the NH_2 species does not appear to be very stable. The NH_2 either undergoes hydrogenation to NH_3 or dehydrogenation to the more stable NH. Since the NH_3 formation peak from H_2NCHO decomposition extends past 425 K while NH_3 desorption from adsorbed NH_3 is complete by 425 K, NH_2 seems more stable

than NH_3 on Rh(111). Thus, the relative adsorption bonding strengths of NH_x species on Rh(111) appears to be: $NH > NH_2 > NH_3$, while the relative stability of the species against losing or gaining a hydrogen appears to be: $NH_3 > NH > NH_2$.

This ordering aids in the understanding of NH_3 decomposition. In the activated decomposition of NH_3 , NH_3 may first lose just one hydrogen to form NH_2 . It appears from this work that the NH_2 would be able to readily accept another hydrogen to reform NH_3 or lose a second hydrogen to form NH . If the second hydrogen is lost and NH is formed, the NH is stable and will not accept another hydrogen or readily lose one. The decomposition of the NH_3 may then be limited by the ability of the surface to remove the final hydrogen.

The temperature at which NH_3 decomposition over Pt foils and Pt(111) begins to occur is ~ 450 K [21,28], the temperature at which the NH species is no longer stable on Rh(111). Assuming a similarity between Rh and Pt which often behave similarly catalytically, this supports the suggestion that the activated decomposition of NH_3 is limited by the decomposition of NH .

5. Summary

H_2NCHO decomposes completely on Rh(111) to form CO , H_2 , N_2 , and NH_3 . The absence of any CN bond retention demonstrates that CO bond formation is favored over CN bond formation on Rh(111). Because of this, it does not appear that N-CO bond containing molecules will be good precursors for HCN synthesis on noble metals. This also suggests that the limiting step in CN bond oxidation is the insertion of the oxygen into the CN containing molecule. In H_2NCHO decomposition, CO desorption is due to the desorption of CO surface fragments. H_2 desorption is caused by both the recombination of H adatoms at ~ 270 K and from decomposition of a surface fragment at ~ 450 K. From mass balances and D_2NCHO experiments, this stable surface fragment has been determined to be NH . The stability of this NH surface species

suggests that NH decomposition may be the limiting factor in the activated decomposition of NH_3 . The N_2 from H_2NCHO decomposition is formed by the recombination of N adatoms. The NH_3 desorption from H_2NCHO decomposition is reaction-limited and appears to be due to the rehydrogenation of NH_2 surface fragments. The amount of nitrogen forming NH_3 ranges from less than 10% at low coverages to over 25% at saturation.

N_2H_4 decomposes completely on Rh(111) to form N_2 , H_2 , and NH_3 . N_2 desorbs in two peaks, one at 270 K which is caused by the decomposition of an N_2H_y ($y \leq 3$) species, and another at 700 K which is due to the recombination of N adatoms. The H_2 desorbs in two peaks, one due to the recombination of H adatoms, and another which is similar to the reaction-limited formation of H_2 following H_2NCHO decomposition and has been assigned to the decomposition of an NH surface species. The NH_3 from N_2H_4 desorbs in two reaction-limited peaks, one due to the intramolecular decomposition of N_2H_4 , and another which, like the NH_3 formation reaction following H_2NCHO decomposition, appears to be due to the rehydrogenation of NH_2 .

References

- [1] S.Y. Hwang, E.G. Seebauer and L.D. Schmidt, Surf. Sci. 188 (1987) 219.
- [2] S.Y. Hwang, A.C.F. Kong and L.D. Schmidt, Surf. Sci. 217 (1989) 179.
- [3] S.Y. Hwang and L.D. Schmidt, J. Phys. Chem. 93 (1989) 8334.
- [4] S.Y. Hwang and L.D. Schmidt, J. Phys. Chem. 93 (1989) 8327.
- [5] J.E. Parmeter, U. Schwalke and H.W. Weinberg, J. Am. Chem. Soc. 110 (1988) 53.
- [6] J.E. Parmeter, U. Schwalke and W.H. Weinberg, J. Vac. Sci. Technol. A 6 (1988) 847.
- [7] J.E. Parmeter, U. Schwalke and W.H. Weinberg, J. Am. Chem. Soc. 109 (1987) 5083.
- [8] J.E. Parmeter, U. Schwalke and W.H. Weinberg, J. Am. Chem. Soc. 109 (1987) 1876.
- [9] C.R. Flores, Q. Gao and J.C. Hemminger, Abstract AVS National Symposium (1989).
- [10] H.H. Sawin and R.P. Merrill, J. Chem. Phys. 73 (1980) 996.
- [11] B.J. Wood and H. Wise, J. Catal. 39 (1975) 471.

- [12] J. Prasad, T. Rufael, E.A. Slaughter and J.L. Gland, *Langmuir*, in press.
- [13] J.L. Gland, G.B. Fisher and G.E. Mitchell, *Chem. Phys. Lett.* 119 (1985) 89.
- [14] W.M. Daniel and J.M. White, *Surf. Sci.* 171 (1986) 289.
- [15] G.A. Papapolymerou and L.D. Schmidt, *Langmuir* 3 (1987) 1098.
- [16] D.W. Johnson and M.W. Roberts, *J. Electron Spectrosc. Relat. Phenom.* 19 (1980) 185.
- [17] M. Grunze, *Surf. Sci.* 81 (1979) 603.
- [18] M. Kiskinova and D.W. Goodman, *Surf. Sci.* 109 (1981) L555.
- [19] A. Vavere and R.S. Hansen, *J. Catal.* 69 (1981) 158.
- [20] C. Egawa, S. Naito and K. Tamaru, *Surf. Sci.* 138 (1984) 279.
- [21] J.L. Gland and E.B. Kollin, *Surf. Sci.* 104 (1981) 478.
- [22] I.C. Bassignana, K. Wagemann, J. Küppers and G. Ertl, *Surf. Sci.* 175 (1986) 22.
- [23] B.A. Morrow and I.A. Cody, *J. Catal.* 45 (1976) 151.
- [24] D.G. Loffler and L.D. Schmidt, *J. Catal.* 41 (1976) 440.
- [25] G.B. Fisher, *Chem. Phys. Lett.* 79 (1981) 452.
- [26] B.A. Sexton and G.E. Mitchell, *Surf. Sci.* 99 (1980) 523.
- [27] C. Benndorf and T.E. Madey, *Surf. Sci.* 135 (1983) 164.
- [28] S.T. Ceyer and J.T. Yates, Jr., *Surf. Sci.* (1985) 584.
- [29] K.K. Al-Shammeri and J.M. Saleh, *J. Phys. Chem.* 90 (1986) 2906.
- [30] J.L. Gland, B.A. Sexton and G.E. Mitchell, *Surf. Sci.* 115 (1982) 623.
- [31] J.L. Gland, G.C. Woodard and V.N. Korchak, *J. Catal.* 61 (1980) 543.
- [32] J.L. Gland and V.N. Korchak, *J. Catal.* 53 (1978) 9.
- [33] T. Pignet and L.D. Schmidt, *J. Catal.* 40 (1975) 212.
- [34] T. Pignet and L.D. Schmidt, *Chem. Eng. Sci.* 29 (1974) 1123.
- [35] J.T. Yates, Jr., P.A. Thiel and W.H. Weinberg, *Surf. Sci.* 84 (1979) 427.
- [36] D.G. Castner, B.A. Sexton and G.A. Somorjai, *Surf. Sci.* 71 (1978) 519.
- [37] A.B. Anton, N.R. Avery, T.E. Madey and W.H. Weinberg, *J. Chem. Phys.* 85 (1986) 507.
- [38] T.W. Root, L.D. Schmidt and G.B. Fisher, *Surf. Sci.* 134 (1983) 30.
- [39] J. Kiss and F. Solymosi, *Surf. Sci.* 135 (1983) 243.